Energy Proceedings
Vol 40, 2024
ISSN 2004-2965

Prediction the Moisture Content of Corn Straw, Wheat Straw and Rice Straw Based on Near Infrared Spectroscopy

Jiale Duan[1], Changqing Dong[1,2,*], Junjiao Zhang[3], Xiaoying Hu[1], Junjie Xue[1], Ying Zhao[1], Xiaoqiang Wang[1]

1 National Engineering Laboratory for Biomass Power Generation Equipment, School of New Energy, North China Electric Power University, Beijing 102206, China

2 State Key Laboratory of Alternate Electrical Power System with Renewable Energy Sources, North China Electric Power University, Beijing 102206, China

3 School of Energy, Power and Mechanical Engineering, North China Electric Power University, Beijing 102206, China
(*Corresponding Author: dongcq@ncepu.edu.cn)

ABSTRACT

The calorific value of biomass fuels is affected by the moisture content. In this study, the moisture content in corn straw, wheat straw, and rice straw was measured and predicted based on near-infrared spectroscopy (NIR) data. The prediction performance of the partial least squares (PLS) model was the best when first-order derivative preprocessing and the stochastic method of dataset division were used at the same time. The correlation coefficient of calibration (R_c^2), the root mean square error of calibration (RMSEC), and the root mean square error of prediction (RMSEP) were 0.937, 1.984 and 3.411 respectively. The results showed that PLS model based on NIR has the potential to rapidly characterize the moisture content of biomass fuel.

Keywords: Moisture, Straw, Biomass, Near infrared spectroscopy

1. INTRODUCTION

The influence of moisture content in biomass fuel has drawn a lot of attention for the thermochemical conversion processes. Excessive moisture content will reduce the calorific value of fuel and increase the cost of the process [1,2]. In addition to this, biomass fuels with unknown moisture may lead to unstable and inefficient combustion process, such as leading to lower efficiency and higher NO_X, CO and PM emissions [3]. Near-infrared spectroscopy is an optical method based on the interaction between electromagnetic waves and matter in the range of 780-2526nm [4-6].

Mora [7] used near-infrared hyperspectral imaging to estimate the moisture content of loblolly pine wood discs, and established a nonlinear iterative partial least squares (NIPALS-PLS) model. The correlation coefficient of the prediction model reached 0.77, and the root mean square errors is 2.1%. Giuseppe [8] used a hand-held near-infrared spectrometer to test the moisture content of 817 wood chip samples from a biomass power plant, and found that the PLS model established by the second-order derivative, 5-point window, second-order polynomial and SNV pretreatment has higher accuracy, and R^2 is 0.89, RMSEP is 3.0%. Jin [9] established a partial least squares model for determining the chemical composition of rice straw by near-infrared spectroscopy. In the experiment, the rice straw sample was ground to 40-60 mesh particles, and the results showed that the R^2 of the model was higher than 0.85. Xue [10] used two different spectrometers to study the influence of near-infrared spectrum acquisition parameters on the spectral repeatability of online measurement of crop straw fuel characteristics. In the experiment, the straw samples were cut shorter than 50mm.

In this paper, in order to ensure the integrity of corn straw, wheat straw and rice straw as much as possible without destroying their internal structure, the samples were cut to less than 30mm for experimental analysis. The aim of this study was to evaluate the potential of NIR spectroscopy in predicting the moisture content of straw-based biomass.

2. MATERIALS AND METHODS

2.1 Sample preparation

This is a paper for 15th International Conference on Applied Energy (ICAE2023), Dec. 3-7, 2023, Doha, Qatar.

Straw samples were taken from Biomass Power Plants across China. A total of 204 straw samples were collected, including 135 corn straws, 45 wheat straws and 24 rice straws. Before analysis, straw samples were cut to a length of less than 30mm with scissors, and the samples were stored in 120mm*170mm sealed bags at room temperature at 20°C.

2.2 Moisture analysis

Moisture data was obtained by classical analysis methods. First, 5g ± 0.5g of a sample with a length of ≤ 30mm (accurate to 0.01g) was weighed in the pre-dry weighed tray. Then, the tray containing the samples was placed into an air-dry oven at 105°C ± 2°C, and dried for 2.5 h under blast conditions. The sample was removed and weighed while hot to avoid moisture absorption by the sample and tray. Finally, inspection drying was carried out, with each drying session lasting 30 minutes, until the mass reduction after two consecutive dryings did not exceed 0.02g or the mass increased. The total moisture content was calculated from the corresponding sample loss mass.

2.3 NIR spectra acquisition

The near-infrared spectrum of each straw sample was collected using a portable biomass fuel analyzer with a wavelength range of 908–1690 nm. Before the spectrum of straw samples was collected, it was necessary for the environmental background value and reference value to be measured first, and then the spectral data of the sample was collected.

2.4 Data processing and analysis

Spectra were processed and screened using a number of different preprocessing methods, including standard normal variation (SNV), multiple scatter correction (MSC), first and second derivatives. And the spectrum without preprocessing method was used as a control. The wavelengths with correlation coefficients greater than the threshold were selected to participate in the model calculation. By setting the threshold range between 0 and 1, with a step size of 0.01, the threshold that minimizes the root mean square error of prediction (RMSEP) of the model is selected as the optimal threshold. In the selection of calibration set and prediction set, three different division methods are adopted, namely random method, K-S method and SPXY method. The division ratio of calibration set and prediction set for each division method was 4:1.

2.5 Results and discussion

The complete sample set of three kinds of straw biomass samples including corn straw, wheat straw and rice straw, and their moisture statistical parameters are shown in Table 1. The moisture content of straw biomass ranged from 9.63% to 70.20%, indicating that the samples in the sample set had a wide range of moisture and were highly representative.

Table 1 - Straw moisture statistical parameters

Index	Max（%）	Min（%）	Mean（%）
Moisture	70.20	9.63	19.78

The near-infrared raw spectra of corn straw, wheat straw and rice straw were shown in Fig. 1 and the average raw spectra were shown in Fig. 2. It can be seen that there were three obvious absorption peaks in the 908-1690nm interval. The first peak was near the wavelength of 960nm, which corresponds to the

Table 2 – CC-MLR modeling analysis

Preprocessing method	Threshold	Number of wavelengths	Data partition method	Calibration		Prediction	
				R_c^2	RMSEC	R_p^2	RMSEP
—	0.24	50	Random	0.935	2.020	0.897	3.655
	0.36	17	K-S	0.893	3.082	0.870	1.665
	0.33	20	SPXY	0.909	2.907	0.185	1.928
SNV	0.20	80	Random	0.910	2.370	0.854	4.357
	0.38	13	K-S	0.734	4.811	0.741	2.936
	0.32	28	SPXY	0.842	3.675	0.804	2.760
MSC	0.39	9	Random	0.668	4.553	0.504	8.019
	0.34	24	K-S	0.717	4.955	0.624	3.545
	0.34	24	SPXY	0.709	5.096	0.551	2.489
1-D	0.22	45	Random	0.936	1.991	0.908	3.450
	0.48	28	K-S	0.926	2.570	0.855	1.687
	0.75	16	SPXY	0.908	2.869	0.838	1.550
2-D	0.12	54	Random	0.935	2.007	0.901	3.574
	0.28	14	K-S	0.891	3.127	0.848	1.735
	0.31	11	SPXY	0.890	3.163	0.546	1.836

second-order double frequency of the stretching vibration of the O-H bond in the water molecule. The second peak was near the wavelength of 1440nm, which corresponds to the first-order frequency doubling of the O-H bond stretching vibration in water molecules. The third peak was around 1650nm, which was related to the first-order frequency doubling of the C-H bond.

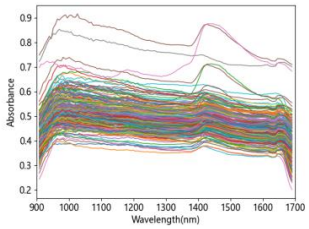

Figure 1 Raw spectrum

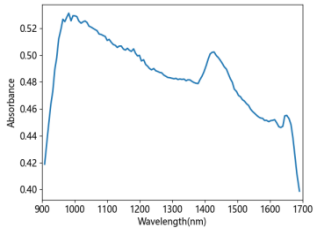

Figure 2 Averaged raw spectrum

The results of multiple linear regression modeling using different preprocessing methods, correlation coefficient method to select characteristic wavelengths and three data division methods were shown in Table 2. The first-order derivative preprocessing method showed the best model performance, the correlation coefficient of calibration R_c^2 reached above 0.908, and the correlation coefficient of prediction R_p^2 reached above 0.838. The prediction graph and residual graph of the multiple linear regression model after first-order derivative preprocessing were shown in Fig.3. Comparing the prediction graphs and residual graphs of the three data division methods, the predicted values of the calibration sets divided by the K-S method and the SPXY method deviate greatly from the reference values, resulting in an increase in the error of the calibration model. The prediction effect of the data set divided by the random method was the best, but it can be seen from the residual graph in Fig. 3(b) that there were still data points with large residuals on the calibration set and prediction set.

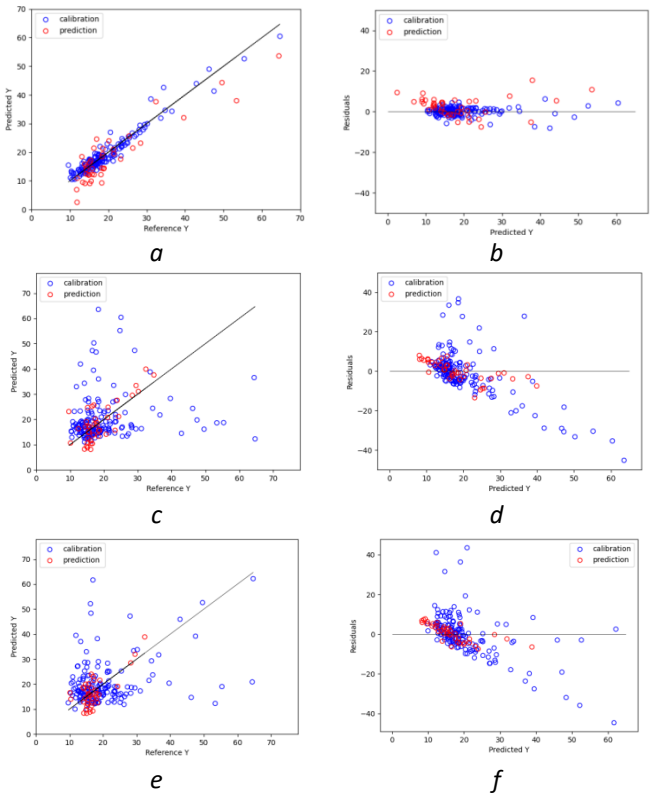

Figure 3 The multiple linear regression model after the first-order derivative preprocessing: the random method predicts the scatter plot (a) and the residual plot (b); the K-S method predicts the scatter plot (c) and the residual plot (d); Scatter plot (e) and residual plot (f) of SPXY method predictions.

Table 3 – CC-PLS modeling analysis

Preprocessing method	Threshold	PLS factors	Data partition method	Calibration		Prediction	
				R_c^2	RMSEC	R_p^2	RMSEP
—	0.16	11	Random	0.932	2.045	0.916	3.299
	0.17	5	K-S	0.900	3.002	0.843	1.656
	0.17	6	SPXY	0.910	2.872	0.694	1.533
SNV	0.24	14	Random	0.878	2.759	0.835	4.620
	0.11	8	K-S	0.815	3.951	0.810	2.944
	0.23	7	SPXY	0.801	4.120	0.848	2.449
MSC	0.31	6	Random	0.705	4.294	0.587	7.320
	0.17	8	K-S	0.766	4.407	0.658	4.419
	0.08	7	SPXY	0.727	4.931	0.718	2.407
1-D	0.21	12	Random	0.937	1.984	0.910	3.411
	0.19	5	K-S	0.924	2.592	0.860	1.570
	0.19	4	SPXY	0.914	2.792	0.771	1.377
2-D	0.11	11	Random	0.937	1.985	0.905	3.509
	0.33	5	K-S	0.872	3.403	0.783	1.817
	0.07	4	SPXY	0.903	2.944	0.834	1.652

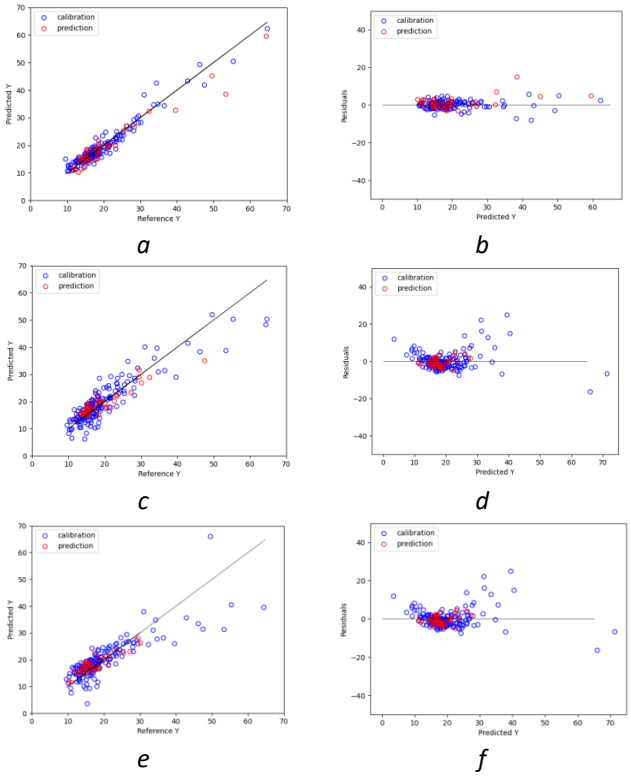

Figure 4 Partial least squares models after first derivative preprocessing: Random method predicts scatter plot (a) and residual plot (b); K-S method predicts scatter plot (c) and residual plot (d); SPXY method predicted scatter plot (e) and residual plot (f).

The partial least squares modeling results after using the correlation coefficient method to select the characteristic wavelength under different preprocessing methods were shown in Table 3. The best prediction effect was achieved after the first derivative preprocessing for different preprocessing methods, with the correlation coefficient of calibration R_c^2 reaching more than 0.914, and the correlation coefficient of prediction R_p^2 reaching more than 0.771. The prediction graph and residual graph of the partial least squares model after first-order derivative preprocessing were shown in Fig.4. The correlation coefficient of prediction set divided by the K-S method and the SPXY method was relatively large, resulting in unstable modeling results.

Compared with the optimal modeling results of the multiple linear regression model, the partial least squares model of the data set divided by the random method after the first-order derivative preprocessing was more accurate, and the correlation coefficient of prediction RMSEP was reduced by 0.039. Based on the information shown in Fig. 3(b) and Fig. 4(b), significant discrepancies can be observed between the calibration set samples and the verification set samples within the predicted moisture range of 35-70%. The relatively weak predictive performance of the model in this range was attributed to the limited number of samples concentrated in this moisture interval.

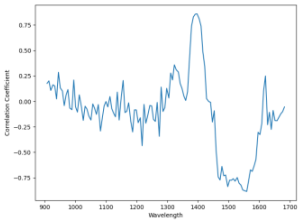

Figure 5 Correlation coefficient plot after first derivative processing.

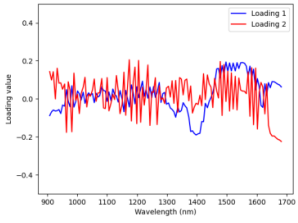

Figure 6 Loading line plot of the best PLS model for moisture prediction.

As shown by the correlation coefficient plot (Fig 5) and the first loading line (Fig 6), two peaks appear continuously in the wavelength range of 1380-1590nm, indicating that the correlation between the spectral absorbance and moisture in this wavelength range was the best strong, this interval corresponds to the secondary frequency doubling (1540nm) of the O-H stretching transformation. The second loading line (Fig 6) has absorption peaks at 950-980nm and 1150-1250nm, which related to the second-order double frequency (960nm) and combined frequency absorption band (1220nm) of O-H bond stretching vibration. Therefore, the strongest correlations between spectral properties and moisture content were found in the intervals 950-980 nm, 1150-1250 nm, and 1380-1590 nm, which has a positive effect on further improving the prediction accuracy.

2.6 Conclusions

In this study, the moisture content of corn straw, wheat straw and rice straw were predicted based on near-infrared spectroscopy, and the influence of various preprocessing methods and data division methods on the prediction model was compared. The prediction performance of the partial least squares (PLS) model was the best when first-order derivative preprocessing and the stochastic method of dataset division were used at the same time. By selecting spectral bands that were strongly correlated with moisture, the prediction accuracy of the model should be improved further.

REFERENCE

[1] Toscano G, Duca D, Pedretti EF, et al. Investigation of woodchip quality: Relationship between the most important chemical and physical parameters. Energy 2016;106:38–44.

[2] Barontini M, Crognale S, Scarfone A, et al. Airborne fungi in biofuel wood chip storage sites. International Biodeterioration & Biodegradation 2014;90:17–22.
[3] Koppejan J, Van Loo S. The handbook of biomass combustion and co-firing. 2008.
[4] Gong YM, Zhang W. Recent progress in NIR spectroscopy technology and its application to the field of forestry. Spectroscopy and Spectral Analysis 2008;28(7):1544–1548.
[5] Skvaril J, Kyprianidis KG, Dahlquist E. Applications of near-infrared spectroscopy (NIRS) in biomass energy conversion processes: A review. Applied Spectroscopy Reviews 2017;52(8):675–728.
[6] Leblon B, Adedipe O, Hans G, et al. A review of near-infrared spectroscopy for monitoring moisture content and density of solid wood. The Forestry Chronicle 2013;89(5):595–606.
[7] Mora C, Schimleck L, Yoon SC, et al. Determination of basic density and moisture content of loblolly pine wood disks using a near infrared hyperspectral imaging system. Journal of Near Infrared Spectroscopy 2011;19(5):401–409.
[8] Toscano G, Leoni E, Gasperini T, et al. Performance of a portable NIR spectrometer for the determination of moisture content of industrial wood chips fuel. Fuel 2022;320:123948.
[9] Jin SY, Chen HZ. Near-infrared analysis of the chemical composition of rice straw. Industrial Crops and Products 2007;26(2):207–211.
[10] Xue JJ, Yang ZL, Han LJ, et al. Study of the influence of NIRS acquisition parameters on the spectral repeatability for on-line measurement of crop straw fuel properties. Fuel 2014;117:1027–1033.